

## Cooperativity scale

***Citation for published version (APA):***

Kulkarni, C., Meijer, E. W., & Palmans, A. R. A. (2017). Cooperativity scale: a structure-mechanism correlation in the self-assembly of benzene-1,3,5-tricarboxamides. *Accounts of Chemical Research*, 50(8), 1928-1936.  
<https://doi.org/10.1021/acs.accounts.7b00176>

***DOI:***

[10.1021/acs.accounts.7b00176](https://doi.org/10.1021/acs.accounts.7b00176)

***Document status and date:***

Published: 15/08/2017

***Document Version:***

Publisher's PDF, also known as Version of Record (includes final page, issue and volume numbers)

***Please check the document version of this publication:***

- A submitted manuscript is the version of the article upon submission and before peer-review. There can be important differences between the submitted version and the official published version of record. People interested in the research are advised to contact the author for the final version of the publication, or visit the DOI to the publisher's website.
- The final author version and the galley proof are versions of the publication after peer review.
- The final published version features the final layout of the paper including the volume, issue and page numbers.

[Link to publication](#)

***General rights***

Copyright and moral rights for the publications made accessible in the public portal are retained by the authors and/or other copyright owners and it is a condition of accessing publications that users recognise and abide by the legal requirements associated with these rights.

- Users may download and print one copy of any publication from the public portal for the purpose of private study or research.
- You may not further distribute the material or use it for any profit-making activity or commercial gain
- You may freely distribute the URL identifying the publication in the public portal.

If the publication is distributed under the terms of Article 25fa of the Dutch Copyright Act, indicated by the "Taverne" license above, please follow below link for the End User Agreement:

[www.tue.nl/taverne](http://www.tue.nl/taverne)

***Take down policy***

If you believe that this document breaches copyright please contact us at:

[openaccess@tue.nl](mailto:openaccess@tue.nl)

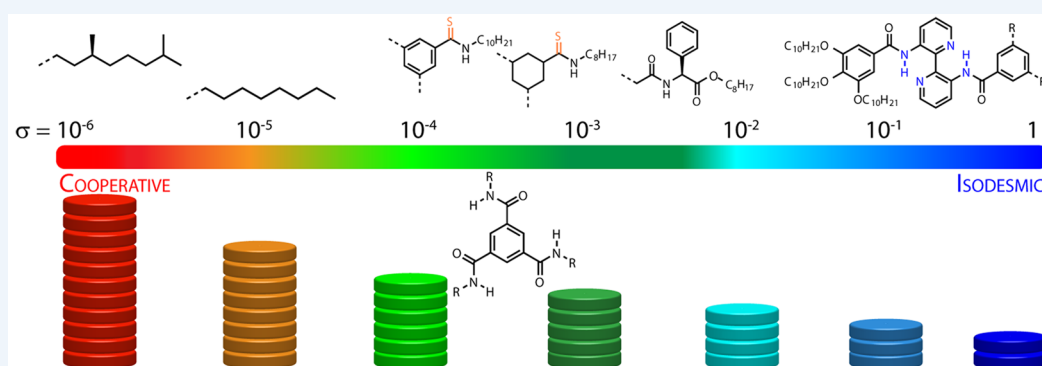
providing details and we will investigate your claim.

## Cooperativity Scale: A Structure–Mechanism Correlation in the Self-Assembly of Benzene-1,3,5-tricarboxamides

Chidambar Kulkarni, E. W. Meijer,\*<sup>1b</sup> and Anja R. A. Palmans\*<sup>1b</sup>

Laboratory of Macromolecular and Organic Chemistry and Institute for Complex Molecular Systems (ICMS), Eindhoven University of Technology, PO Box 513, 5600 MB Eindhoven, The Netherlands

### Supporting Information



**CONSPECTUS:** The self-assembly of small and well-defined molecules using noncovalent interactions to generate various nano- and microarchitectures has been extensively studied. Among various architectures, one-dimensional (1-D) nano-objects have garnered significant attention. It has become increasingly evident that a cooperative or nucleation–elongation mechanism of polymerization leads to highly ordered 1-D supramolecular polymers, analogous to shape-persistent biopolymers such as actin. With this in mind, achieving cooperativity in self-assembled structures has been actively pursued with significant success. Only recently, researchers are focusing on the origin of the mechanism at the molecular level in different synthetic systems. Taking a step further, a thorough quantitative structure–mechanism correlation is crucial to control the size, shape, and functions of supramolecular polymers, and this is currently lacking in the literature.

Among a plethora of molecules, benzene-1,3,5-tricarboxamides (BTAs) provide a unique combination of important noncovalent interactions such as hydrogen bonding,  $\pi$ -stacking, and hydrophobic interactions, for self-assembly and synthetic ease. Due to the latter, a diverse range of BTA derivatives with all possible structural mutations have been synthesized and studied during the past decade, mainly from our group. With such a large body of experimental results on BTA self-assembly, it is time to embark on a structure–mechanism correlation in this family of molecules, and a first step toward this will form the main focus of this Account. The origin of the cooperative mechanism of self-assembly in BTAs has been ascribed to 3-fold intermolecular hydrogen bonding (HB) between monomers based on density-functional theory (DFT) calculations. The intermolecular hydrogen-bonding interaction forms the central premise of this work, in which we evaluate the effect of different moieties such as alkyl chains, and amino acids, attached to the core amides on the strength of intermolecular HB, which consequently governs the extent of cooperativity (quantified by the cooperativity factor,  $\sigma$ ). In addition to this, we evaluate the effect of amide connectivity (C- vs N-centered), the role of solvents, amides vs thioamides, and finally the influence of the benzene vs cyclohexane core on the  $\sigma$ . Remarkably, every subtle structural change in the BTA monomer seems to affect the cooperativity factor in a systematic and rationalizable way.

The take home message will be that the cooperativity factor ( $\sigma$ ) in the BTA family forms a continuous spectrum from 1 (isodesmic) to  $<10^{-6}$  (highly cooperative) and it can be tuned based on the appropriate modification of the BTA monomer. We anticipate that these correlations drawn from the BTA series will be applicable to other systems in which HB is the main driving force for cooperativity. Thus, the understanding gained from such correlations on a prototypical self-assembling motif such as BTA will aid in designing more complex systems with distinct functions.

### 1. INTRODUCTION

The assembly of small organic molecules using noncovalent interactions such as hydrogen-bonding,  $\pi$ - $\pi$  stacking, and hydrophobic interactions results in long polymeric chains, which are termed as supramolecular polymers.<sup>1</sup> Due to the reversibility of these noncovalent interactions, supramolecular polymers often

display adaptability and self-healing, features not encountered in covalent polymers.<sup>2</sup> As a result, supramolecular polymers have emerged as one of the prominent pillars of polymer science.<sup>3,4</sup>

Received: April 10, 2017

Published: July 10, 2017

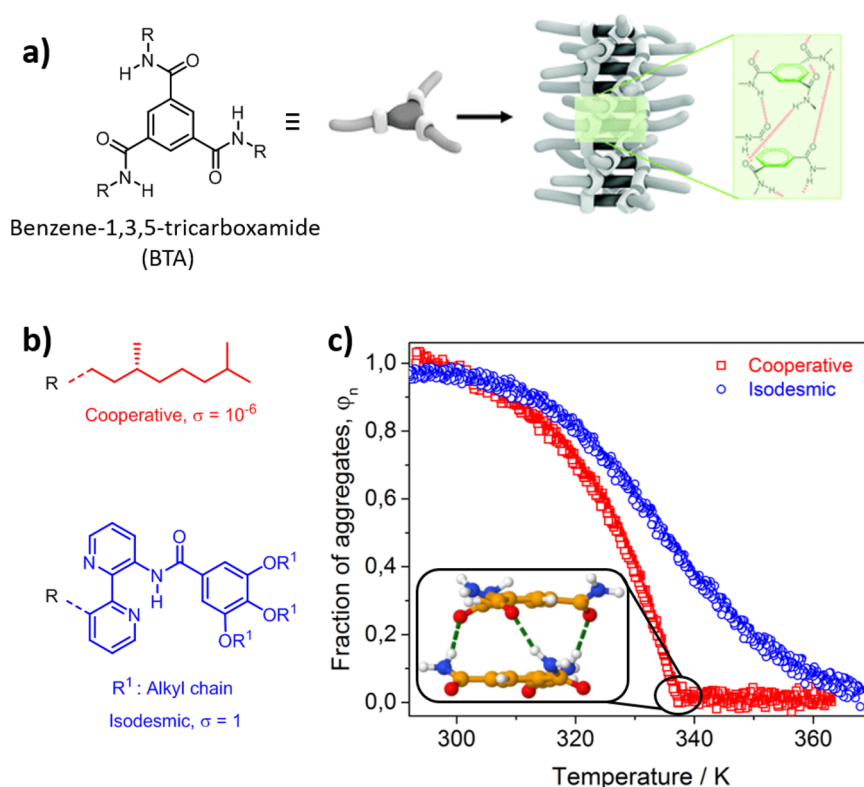


**Figure 1.** (a) Molecular structure of benzene-1,3,5-tricarboxamide (BTA) and a schematic representation of its self-assembly into 1-D helical stacks stabilized by 3-fold intermolecular hydrogen-bonding interactions. (b) BTA derivatives exhibiting isodesmic and cooperative mechanisms based on the substituents on the amide. (c) Typical cooling curves for the two systems shown in panel b (cooperative ( $\square$ ),  $c = 12 \mu\text{M}$  in *n*-heptane; isodesmic ( $\circ$ ),  $c = 50 \mu\text{M}$  in MCH). Inset of panel c shows a model of BTA dimer, which is the likely nucleus for further growth.

The material properties of supramolecular polymers critically depend on (i) the strength of the noncovalent interaction between monomers determining the molecular weight and (ii) the mechanism of polymerization dictating the molar-mass dispersity.<sup>5</sup> In the past decade, the focus of supramolecular polymer research shifted from controlling the strength of supramolecular interactions to studying and understanding the mechanism of supramolecular polymerizations with the aim to regulate supramolecular material properties.

The mechanism of one-dimensional (1-D) supramolecular polymerization is classified into either cooperative/nucleation–elongation or isodesmic.<sup>5</sup> In a cooperative supramolecular polymerization, the assembly is thermodynamically distinguished by two equilibrium constants, one for the less favorable nucleation process ( $K_{\text{nuc}}$ ) and another for the subsequent highly favorable elongation process ( $K_{\text{elo}}$ ). When the nucleus consists of a dimer, this is referred to as the  $K_2$ – $K$  model.<sup>6</sup> In an isodesmic mechanism, all binding constants throughout the course of polymerization are equal (also called the equal  $K$ -model).<sup>7</sup> Cooperative and isodesmic mechanisms are analogous to chain and step-growth mechanisms, respectively, in covalent polymers. These aspects have been reviewed in great detail elsewhere, and thus we refrain from a thorough discussion about the thermodynamic classification of supramolecular polymerization.<sup>5</sup> Nonetheless, it has been consistently observed across many systems that a cooperative mechanism gives rise to high virtual molecular weight polymers with an internally ordered supramolecular structure. It is conjectured that this internal order stems from a well-defined nucleus, on which further polymerization takes place. Moreover, recent examples in the emerging field of living supramolecular polymerization invariably involve a

cooperative mechanism.<sup>8–10</sup> Thus, achieving and understanding cooperative supramolecular polymerizations has received significant attention in the past decade.

A plethora of examples of cooperative 1-D supramolecular polymerizations have been reported.<sup>11</sup> Although a few notable studies exist on relating structure or the noncovalent interaction to the properties of a system in supramolecular chemistry,<sup>12–16</sup> approaches to rationalizing cooperativity have been scarce.<sup>17,18</sup> We envisage that a classical physical–organic chemistry approach to understanding structure–cooperativity correlations will aid in achieving functional 1-D supramolecular polymers with precise size, shape, and properties. Benzene-1,3,5-tricarboxamides (BTAs), a molecular model system for supramolecular polymerization, have been extensively investigated in the past decade by our group and others.<sup>19</sup> The supramolecular polymerization mechanism of several different BTAs has been studied, and it was found that depending on the structure of the monomers the complete spectrum of mechanisms, from isodesmic to highly cooperative, was present (Figure 1). Due to the large body of experimental data on the mechanism of BTA derivatives, it is an ideal hydrogen-bonded supramolecular prototype to attempt a structure–mechanism correlation.

In this Account, we first reconcile the different models used to quantify the cooperativity in a system and then delineate the factors governing cooperativity in the BTA family. Next, we look at the influence of the BTA monomer structure on the cooperativity factor ( $\sigma$ ) by demarcating the structural changes into (i) influence of substitution on the amide nitrogen and (ii) structural changes to the BTA core. Under each section, the effects of structural mutation are elaborated to clearly bring out a structure–mechanism correlation. Finally, we put our work into

perspective with possible future directions to harnessing cooperativity in functional self-assembled materials.

## 2. QUANTIFYING THE THERMODYNAMIC PARAMETERS OF COOPERATIVE SELF-ASSEMBLY

The mechanism of self-assembly in BTAs and other systems in organic solvent has been regularly studied through temperature-dependent UV/vis absorption and circular dichroism (CD) spectroscopy.<sup>20</sup> Typically, the normalized spectroscopic signal (between 0 and 1) at a particular wavelength (characteristic of assembly) is plotted as a function of temperature and the curve is referred to as a “cooling curve”. The cooling curves need to be recorded at slow rates such that no hysteresis is observed, thus ensuring that the system remains under thermodynamic control. Such cooling curves are fitted with mathematical models either based on a thermally activated equilibrium polymerization<sup>21</sup> or by taking the equilibrium between the monomer pool and supramolecular polymers into account and solving the mass-balance equations.<sup>22,23</sup> In both cases, the models describe the self-assembly of a one-component system into a 1-D aggregate and permit one to extract the various thermodynamic parameters that describe the self-assembly process. The thermally activated equilibrium polymerization model assumes the activation of a monomer (characterized by the dimensionless equilibrium constant  $K_a$ ) followed by polymerization (characterized by an energy term  $h_e$ ). The cooling curve is then typically described by two different equations that can be easily fitted to the experimental data using nonlinear regression. A caveat in this methodology is the subjectivity involved in demarking the two processes. In contrast, the mass-balance (MB) model takes into account the exchange of monomers between the polymers and free monomers in solution. The fraction of aggregated species at various temperatures is simulated based on mass-balance equations for different sets of thermodynamic parameters that describe the equilibrium in the nucleation phase ( $K_{nuc}$ , characterized by  $\Delta H_{nuc}$ ,  $\Delta S_{nuc}$ ) and the equilibrium in elongation phase ( $K_{elo}$ , characterized by  $\Delta H_{elo}$ ,  $\Delta S_{elo}$ ), in which the two phases are separated by the characteristic temperature  $T_c$ . Often  $\Delta S_{elo}$  is taken as equal to  $\Delta S_{nuc}$  to facilitate the fitting procedure. The best match to the experimental curve is the fitted curve. It is recommended to fit cooling curves at multiple concentrations

simultaneously to obtain accurate values for the thermodynamic parameters. The extent of cooperativity in the MB model is quantified through the expression,  $\sigma = K_{nuc}/K_{elo} = \exp(\Delta H_{np}/(RT))$  in which  $\Delta H_{np}$  is the nucleation penalty assuming  $\Delta S_{elo} = \Delta S_{nuc}$ . The more negative the value of  $\Delta H_{np}$  (defined as  $(\Delta H_{elo} - \Delta H_{nuc})$ ), the smaller the  $\sigma$ -value becomes and hence higher the cooperativity in the system. In case of  $\Delta H_{elo}$  equals  $\Delta H_{nuc}$ ,  $\sigma$  equals 1, which signifies an isodesmic process. Although in several of our previous publications the  $K_a$  and  $h_e$  have been quantified for BTAs, in this work, we focus on the  $\sigma$ -values (at 293 K) derived from the MB model.

## 3. MOLECULAR ORIGIN OF THE COOPERATIVITY IN BENZENE-1,3,5-TRICARBOXAMIDES

BTAs form triple helical hydrogen-bonded (HB) 1-D structures (Figure 1a) in their crystalline form.<sup>24</sup> A typical cooling curve for (R)-1 BTA recorded in *n*-heptane at dilute concentrations indicates a nonsigmoidal behavior with a critical temperature below which elongation takes place (Figure 1c). Fitting the data with the MB model yields  $\sigma = 5.7 \times 10^{-7}$ , indicating high cooperativity.<sup>25</sup> In order to understand the origin of cooperativity, we performed density functional theory (DFT) based computations on oligomers of BTA.<sup>26</sup> These studies indicated strong triple helical HB between monomers (with a rotational angle of  $60^\circ$  between consecutive monomers) to be the dominant factor in stabilizing an assembly. The most likely size of the nucleus is a dimer (Figure 1c, inset) or trimer.<sup>27</sup> The stabilization energy per monomer ( $\Delta E_{avg} = (E_n - nE_1)/(n - 1)$ ) gained due to oligomerization showed a nonmonotonic decrease (Figure 2a). The change in  $\Delta E_{avg}$  decreases at higher oligomer numbers. This indicates that beyond a certain oligomer size further addition of monomers does not lead to significant stabilization per monomer, and this phenomenon of non-additivity is called cooperativity. In addition, electrostatic potential isosurfaces showed clear charge redistribution along an oligomer, indicating significant polarization (Figure 2b). Thus, the origin of cooperativity in the assembly of BTAs was attributed to the 3-fold intermolecular hydrogen bonding between the monomers. The dihedral angle ( $\theta$ ) between the benzene and amide plane directly influences the hydrogen-bond strength in an oligomer. Since it is very difficult to quantify the strength of

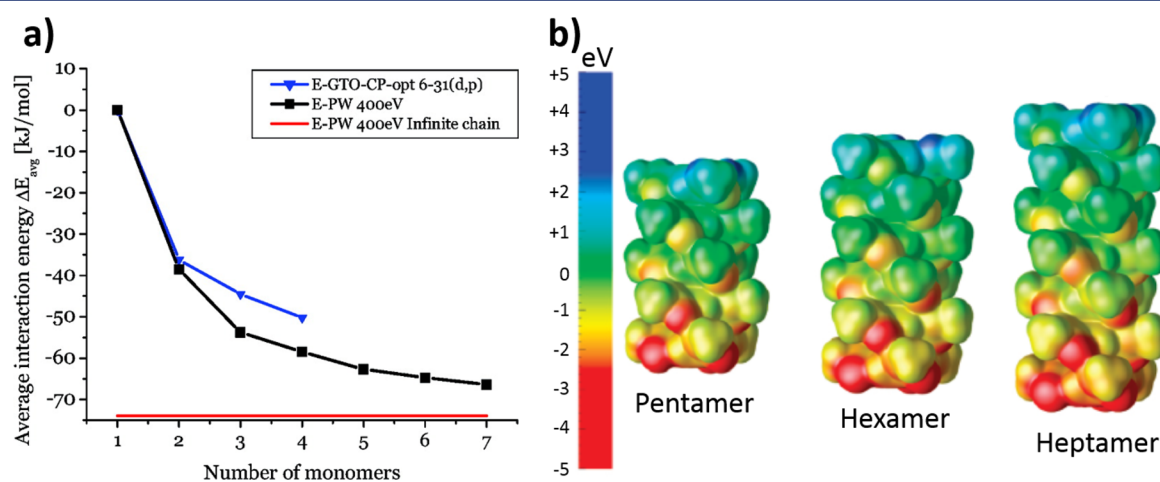


**Figure 2.** (a) Computed stabilization energy per monomer ( $\Delta E_{avg} = (E_n - nE_1)/(n - 1)$ ) as a function of oligomer size ( $n$ ) for BTA model compound (alkyl chains replaced by methyl groups on amide). Legends indicate the different levels of theory used for computation. (b) Electrostatic potential in eV plotted on isodensity surfaces of  $10^{-5} \text{ e}/\text{\AA}^3$  obtained using plane-wave (PW) density functional theory studies of BTA model compound. Reproduced with permission from ref 26. Copyright 2010 American Chemical Society.



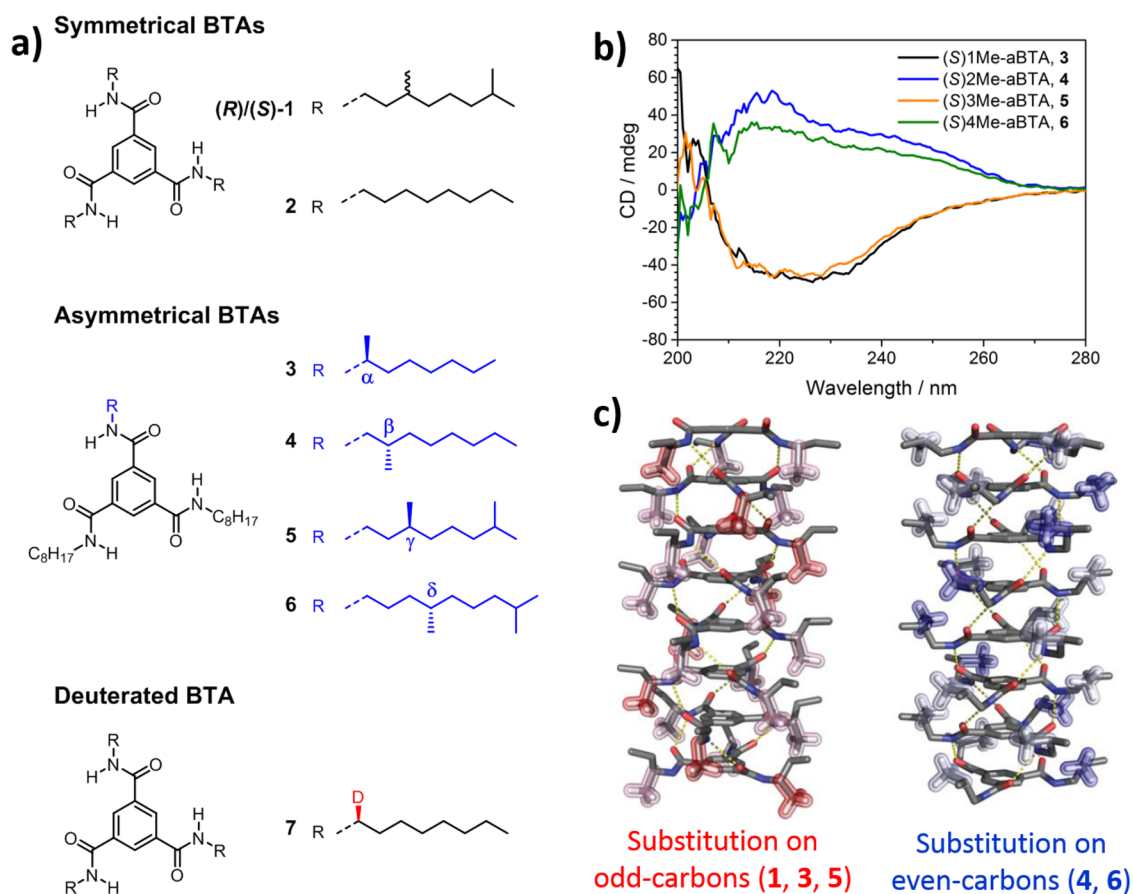


**Figure 3.** Effect of different alkyl chains: (a) Structure of symmetrical, asymmetrical, and deuterated BTAs. For BTA 1, both (S) and (R) enantiomers have been studied, and the stereochemistry is explicitly mentioned in the manuscript. For all the other BTA derivatives, only the (S)-enantiomer was studied, and thus the stereochemistry is not explicitly mentioned. (b) CD spectra of asymmetrical BTAs (aBTAs) at 20 °C in MCH ( $c = 30 \mu\text{M}$ ). (c) The structure of a model BTA octamer exhibiting the difference between the substitution on the odd and even numbered carbon atom of the side chain. Reproduced with permission from ref 29. Copyright 2012 Royal Society of Chemistry.

hydrogen bonding, we use  $\theta$  and hydrogen-bond length as a measure to understand the influence of different substituents on  $\sigma$ .

#### 4. INFLUENCE OF SUBSTITUENTS ON THE AMIDE NITROGEN ON COOPERATIVE SELF-ASSEMBLY

##### 4.1. Linear and Branched Alkyl Chains

Of all the possible mutations to the BTA, variations on the amide nitrogen are the most obvious and convenient due to the synthetic accessibility of different amines.<sup>25,28–30</sup> The first detailed quantitative work on the mechanisms of self-assembly in the BTA family was carried out on  $C_3$ -symmetric BTAs (R)-1 and 2 (Figure 3) using CD or UV/vis spectroscopy or both at dilute concentrations in *n*-heptane as solvent.<sup>25</sup> CD spectroscopy showed an exciton-coupled bisignate Cotton effect for the  $n \rightarrow \pi^*$  transition for (R)-1 in *n*-heptane and MCH, indicative of a helical arrangement of the hydrogen-bonding array. Cooling curves obtained from both CD and UV/vis measurements in MCH exhibited a critical point in the self-assembly process and were fitted with the MB model to derive the various thermodynamic parameters of self-assembly. A similar analysis on 2 using UV/vis studies also indicated a cooperative self-assembly. Interestingly, the  $\sigma$  for (R)-1 is 2 orders of magnitude smaller than that for 2 (Table 1 and *vide infra*).

In addition to the symmetric BTAs, we have also investigated asymmetric BTAs (3–6) comprising two *n*-octyl chains and one chiral side chain on the amides (see Figure 3).<sup>28</sup> The stereogenic

**Table 1.** Cooperativity Factor ( $\sigma$ ) for BTAs 1–7 in MCH and *n*-Heptane<sup>a</sup>

BTA	$\sigma$ in MCH	$\sigma$ in <i>n</i> -heptane
(R)-1	$3.7 \times 10^{-6}$ ( $3.0 \times 10^{-6}$ )	$5.7 \times 10^{-7}$
2	$(3.8 \times 10^{-4})$	$(1.5 \times 10^{-5})$
3	$<10^{-8}$	$<10^{-8}$
4	$1.9 \times 10^{-6}$	$<10^{-8}$
5	$<10^{-8}$	$<10^{-8}$
6	$3.1 \times 10^{-3}$	$<10^{-8}$
7	$(0.9 \times 10^{-4})$	$(2.5 \times 10^{-5})$

<sup>a</sup>The  $\sigma$  value was calculated at 293 K and obtained by refitting previously published CD cooling curves with the MB model. Values in parentheses are obtained from fits to the UV/vis cooling curves. Very low values for  $\sigma$  could not be determined accurately; thus all  $\sigma$  values lower than  $10^{-8}$  are not compared and designated as  $<10^{-8}$ .

methyl group was systematically varied from the  $\alpha$  to the  $\delta$  position along the carbon chain to investigate the presence of an odd–even effect. Detailed studies on the BTA series 3–6 revealed that in MCH two types of Cotton effects were observed: for the methyl at the  $\alpha$  and the  $\gamma$  position, a single Cotton effect with a maximum at 223 nm was observed, whereas for the methyl at the  $\beta$  and  $\delta$  position a double Cotton effect was found with a maximum at 216 nm and a shoulder at 242 nm (Figure 3b). TDDFT computations performed on the monomer show that the angle between the C=O and phenyl core dictates the shape

of the CD spectra. A  $\theta$ -value of  $45^\circ$  showed a single Cotton effect, whereas a lower  $\theta$  of  $35^\circ$  showed a double Cotton effect. In fact, the calculated CD spectra reproduced well the two different types of Cotton effects measured experimentally, suggesting that the shape of the CD spectra is indeed strongly dependent on  $\theta$ .

In addition, the influence of  $\theta$  ( $35^\circ$  and  $45^\circ$ ) on the extent of cooperativity in the self-assembly of BTAs 3–6 in MCH was investigated. Interestingly, the  $\sigma$  parameter showed an odd–even effect in MCH (see Table 1); the  $\sigma$  value for BTAs substituted at the  $\alpha$  and  $\gamma$  position was consistently smaller than that of BTAs substituted at the  $\beta$  and  $\delta$  position, indicating a higher cooperativity for the former. Molecular mechanics calculations on an octamer of a model compound showed a perpendicular and parallel orientation of the methyl group on the  $\alpha$  and  $\beta$  carbon atom, respectively (Figure 3c).<sup>29</sup> As a consequence, the inter-ring distance was 3.78 Å for  $\alpha$ -substituted (odd) compared to 3.63 Å for the  $\beta$ -substituted (even) BTAs. This in turn result in an increased  $\theta$  and lower HB distance for perpendicular orientation ( $\alpha$ -substituted) compared to the parallel arrangement of methyl groups ( $\beta$ -substituted). Thus, the perpendicular orientation of the methyl substituent on the odd-carbon atoms subtly changes the  $\theta$ , which is reflected in an increased cooperativity or smaller  $\sigma$ -value.

Based on these results, we expected that achiral 2 would behave like 4 and 6 due to the tighter packing of unbranched linear chains and a diminished  $\theta$  compared to 1, leading to lower cooperativity. Indeed, the UV/vis cooling curves of 2 in MCH show  $\sigma$  of  $3.8 \times 10^{-4}$ , indicating lower cooperativity for the linear chain BTA 2. Further, a selectively deuterated analogue of 3 was prepared, D-BTA 7, to induce excess helicity.<sup>30</sup> Interestingly, 7 showed a double Cotton effect in MCH, indicating a  $\theta$  of  $35^\circ$ , and a  $\sigma$  of  $0.9 \times 10^{-4}$ , which is indeed larger than that observed for (R)-1 in MCH ( $\sigma = 3 \times 10^{-6}$ ) in which  $\theta = 45^\circ$ .

## 4.2. Effect of the Nature of the Alkane Solvent on Cooperativity in Alkyl-Substituted BTAs

Solvents play a pivotal role in most if not all self-assembly processes.<sup>21,31</sup> In the self-assembly of BTA (R)-1, it was found that the  $T_e$ 's in *n*-heptane were significantly higher compared to those in MCH, indicating a higher stability of the formed aggregates in *n*-heptane.<sup>29</sup> In addition, a stronger cooperativity was observed for (R)-1 in *n*-heptane ( $\sigma = 5.7 \times 10^{-7}$ ) compared to that in MCH ( $\sigma = 3.7 \times 10^{-6}$ ). Intriguingly, upon mixing MCH and *n*-heptane in different ratios, the  $T_e$  decreased nonlinearly with the amount of MCH added, indicating that the solvent shows specific interactions and participates actively in the aggregation process.

The cooperativity of the even-substituted BTAs was lower than the odd-substituted ones in MCH, but the  $\sigma$  was identical in *n*-heptane (Table 1). This was attributed to different  $\theta$  in MCH and *n*-heptane (*vide supra*): intercalation of *n*-heptane into the helical aggregates always resulted in a  $\theta$  of  $45^\circ$  for all compounds 3–6, whereas compounds 4 and 6 adopted a lower  $\theta$  of  $35^\circ$  in MCH. This smaller angle is directly reflected in lower cooperativity. In fact, the cooperativity for achiral BTA 2 in MCH ( $\sigma = 3.8 \times 10^{-4}$ ) is lower than that in *n*-heptane ( $\sigma = 1.5 \times 10^{-5}$ ). Interestingly, a similar trend was observed for 7, in which fitting of the UV cooling curves gave  $\sigma = 2.5 \times 10^{-5}$  and  $0.9 \times 10^{-4}$  in *n*-heptane and MCH, respectively (Table 1).<sup>32</sup>

## 4.3. Factors Competing with Intermolecular Hydrogen Bonding

Due to the good compatibility of MCH with many BTA-based systems, in the remainder of this Account, we focus on the results obtained in exclusively MCH. BTAs substituted with 3,3'-diamino-2,2'-bipyridine units on the amide position (Figure 4a) were investigated in apolar solvents.<sup>33</sup> The mechanism of self-assembly of these extended-disc BTAs were

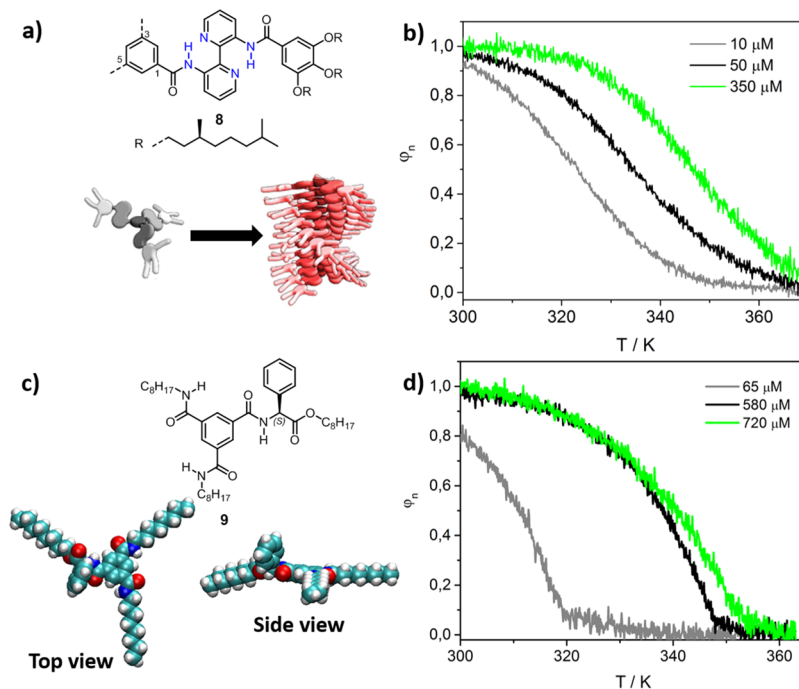


**Figure 4.** (a) Molecular structure of BTA 8. The atoms in blue color engage in intramolecular hydrogen bonding. The substituents on positions 3 and 5 of benzene core are same as that on position 1. A schematic representation of the self-assembly of 8 is shown below the structure. (b) Experimental cooling curves obtained from CD studies of 8 in MCH at different concentrations. (c) Molecular structure of BTA 9 and its 3D-space filling molecular model showing the bulky phenyl groups close to one of the amides. (d) Normalized cooling curves of 9 obtained using CD studies in MCH.

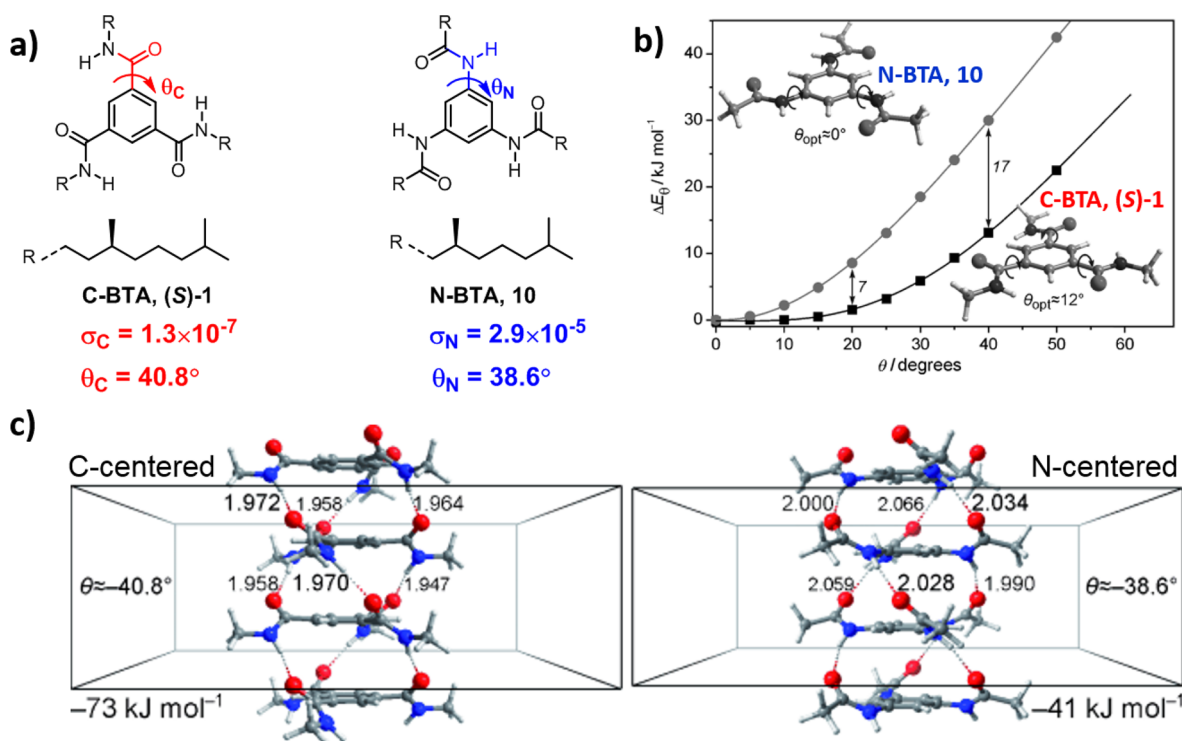


**Figure 5.** (a) Structure of C- and N-centered BTAs (S)-1 and 10. The corresponding  $\sigma$  derived from CD studies and the  $\theta$  are listed below the structures. (b) Potential energy profile around the  $\text{C}_{\text{aromatic}}-\text{C}_{\text{carbonyl}}$  and  $\text{C}_{\text{aromatic}}-\text{C}_{\text{nitrogen}}$  bond for the model compounds of (S)-1 and 10 (chiral alkyl chains replaced by methyl for computational tractability), respectively, at PBE/6-311+g(d,p) level of theory. The values indicated at a particular angle represent the difference in energy between the C- and N-centered BTA. (c) Plane wave DFT optimized structures of model compounds of (S)-1 and 10 showing different hydrogen-bond lengths and  $\theta$ . Reproduced with permission from ref 39. Copyright 2010 Wiley-VCH.

studied in detail using temperature-dependent CD studies.<sup>34</sup> Curiously, the transition from the monomers to assembly for 8 in MCH occurs gradually, and the data is in excellent agreement with the isodesmic model ( $\sigma = 1$ ). The 3,3'-diamino-2,2'-bipyridine connected to the amide nitrogen has been shown to undergo *intramolecular hydrogen bonding* based on  $^1\text{H}$  NMR studies<sup>35</sup> and quantum chemical computations.<sup>34</sup> As a result of the intramolecular hydrogen bonding, the  $\theta$  is 7–13° and the rotation angle between two consecutive monomers in an assembly is 13–15°. Due to these structural parameters, monomers of 8 cannot engage in any intermolecular hydrogen bonding along the stacking direction. Thus, due to the lack of intermolecular hydrogen bonding, 8 self-assembles in an isodesmic manner ( $\sigma = 1$ ).

Also the introduction of a bulky group such as phenylglycine on one of the amides of BTA with *n*-octyl groups on other two (Figure 4c) significantly affects the cooperativity in BTAs.<sup>36</sup> The shape of the Cotton effect for 9 in MCH is similar to that observed of BTA 1, indicating a similar helical packing for 9. Temperature-dependent CD studies resulted in cooling curves with an apparent critical point (Figure 4d). However, fitting the curves with the MB model,<sup>22,23</sup> indicated a significantly weaker cooperativity with  $\sigma = 6.7 \times 10^{-3}$ . 3D-space-filling models of 9 show a considerable amount of steric hindrance around the amide bond due to the phenylglycine (Figure 4c). Thus, to accommodate the bulky phenyl groups, it is likely that the strength of intermolecular hydrogen bonding decreases leading to lowering of the cooperativity in the system. An even more bulky side chain such as phenylalanine seemed to afford an isodesmic supramolecular polymerization.<sup>37</sup> However, studies by the group of Bouteiller indicated that the self-assembly

pattern of BTAs with such bulky substituents showed a change in hydrogen-bond pattern, which inhibited supramolecular polymerization.<sup>38</sup>

## 5. EFFECT OF MUTATIONS IN THE CORE OF BENZENE-1,3,5-TRICARBOXAMIDE ON THE COOPERATIVE SELF-ASSEMBLY

### 5.1. The Influence of Amide Connectivity

The amide connectivity in BTAs can be of two types based on the atom of attachment to the benzene core, C-centered ((S)-1) and N-centered (10, Figure 5a).<sup>39</sup> Oligo(*p*-phenylenevinylene) functionalized N-centered BTA did not show significant intermolecular hydrogen bonding compared to its C-counterpart.<sup>40</sup> Thus, in order to understand the origin of such differences in amide connectivity and if it can affect the mechanism of self-assembly, a detailed experimental and computational study was carried out on the simplest BTAs with chiral side chains ((S)-1 and 10).<sup>39</sup>

The FT-IR and CD studies indicated helical packing for 10. Temperature-dependent CD data when fitted to the MB model indicated a cooperative mechanism,<sup>39</sup> similar to that observed for 1. The  $\sigma$  was found to be  $2.9 \times 10^{-5}$  for 10, 2 orders of magnitude larger than the corresponding C-centered BTA (S)-1. Plane wave DFT studies were carried out on an infinite stack of model compounds of (S)-1 and 10 to understand the difference in the assembly behavior. In the optimized structure of monomer,  $\theta_N$  (N-centered) = 0 and  $\theta_C$  (C-centered) = 12° was obtained. Further, the torsional barrier at  $\theta$  of 40° was found to be 17 kJ/mol higher for N-centered BTA compared to the C-centered BTA (Figure 5b). The hydrogen-bond length was 1.94–1.97 Å and 1.99–2.06 Å for C- and N-centered BTA,



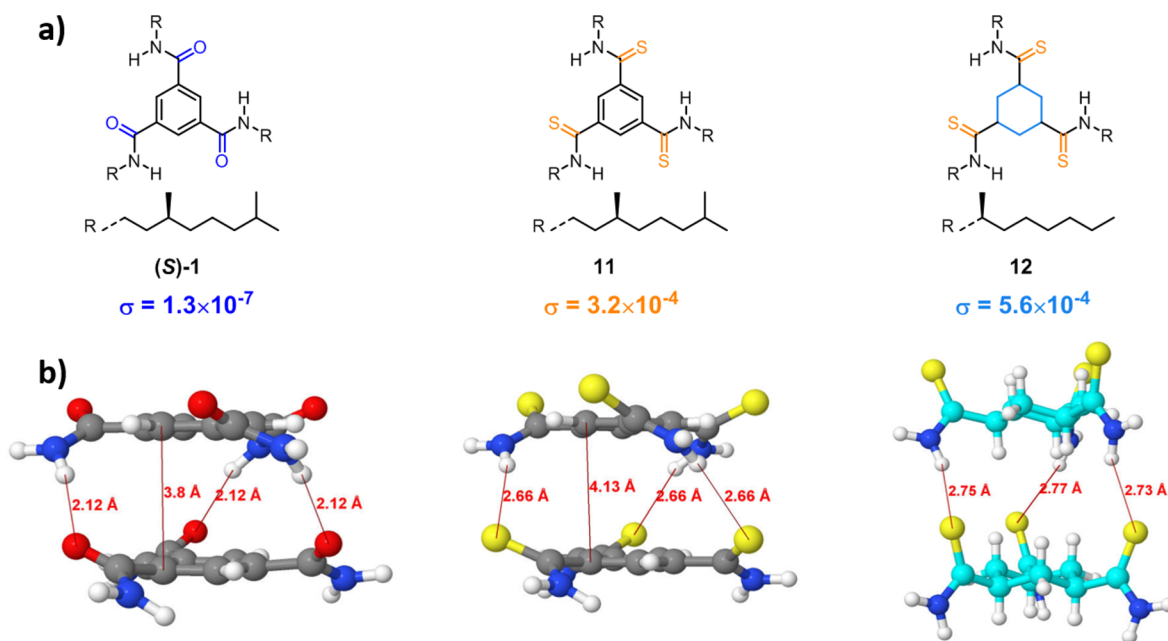


**Figure 6.** (a) Structures of amide ((S)-1), thioamide (11), and cyclohexane–thioamide (12). The  $\sigma$ -values obtained from CD studies (in MCH) for each of the BTAs are mentioned below the structures. (b) DFT based (B3LYP/6-31+g(d,p) level of theory) optimized structures (of dimers) of the corresponding model compounds (alkyl chain replaced by hydrogen). The hydrogen-bond length and  $\pi$ – $\pi$  stacking distances are shown in red color.

respectively, indicating stronger intermolecular hydrogen bonding in the former. Also, the  $\theta$  in the optimized infinite stack for N-centered BTA is lower compared to its C-counterpart ( $\theta_N = 38.6^\circ$  and  $\theta_C = 40.8^\circ$ ) (Figure 5c).<sup>39</sup> All these structural parameters suggest that the lower  $\sigma$  observed for the N-centered BTA (10) is due to the weaker hydrogen bonding brought about by the higher barrier for rotation about the  $C_{\text{aromatic}}-N_{\text{amide}}$  bond compared to the C-centered BTA ((S)-1).

## 5.2. The Effect of Amide versus Thioamide and Benzene versus Cyclohexane Core

Most of the BTA derivatives are based on the ubiquitously found amide bonds. Thioamide motifs incorporated into peptides allow the tuning of the  $\alpha$ -helical structure.<sup>41</sup> To explore the utility of this seldom-studied group in supramolecular chemistry, we have studied the self-assembly of thioamide BTA (11) both in bulk and in dilute alkane solutions (Figure 6).<sup>42</sup>

The FT-IR studies of 11 in bulk and solution state and CD spectroscopy in MCH suggest a helical arrangement in the assembly. Temperature-dependent CD studies of 11 in MCH indicated two distinct phases of self-assembly, namely, nucleation and elongation separated by a critical temperature ( $T_c$ ).<sup>42</sup> The  $\sigma$  for 11 is  $3.2 \times 10^{-4}$ , 3 orders of magnitude larger than the corresponding amide BTA (S)-1. We resorted to computational studies to understand the origin of the difference in the  $\sigma$  value between (S)-1 and 11. The hydrogen-bond length and  $\pi$ – $\pi$  stacking distance for 11 are 2.67 and 4.2 Å, respectively. The corresponding hydrogen-bond length and  $\pi$ – $\pi$  stacking distances for (S)-1 are lower by 0.55 and 0.4 Å, respectively (Figure 6b), indicating the weaker intermolecular hydrogen-bonding for 11 compared to (S)-1. Thus, weaker hydrogen bonding in 11 could be the cause for its lower cooperativity.

The last and the most noticeable mutation to BTA core was carried out by replacing the benzene core of thioamide BTA (11) with the cyclohexane core (cyclohexane-tris(thioamide), CTA, 12) to study the effect of the core on the self-assembly of this class of compounds. The CD cooling curves of 12 in MCH were

fitted to the MB model to extract a  $\sigma$ -value of  $6.4 \times 10^{-4}$ . The  $\sigma$ -value for CTA 12 is twice that for the BTA 11, indicating a slightly lower cooperativity for 12 when compared to 11. DFT calculations on a dimer of CTA model compound show an increased hydrogen-bond length (by  $\sim 0.1$  Å) compared to 11 (Figure 6b). Thus, the lower cooperativity of 12 could be attributed to the weaker hydrogen bonding.

## 6. CONCLUSIONS AND OUTLOOK

Since the first report of cooperative 1-D self-assembly in synthetic systems in 2006,<sup>21</sup> mechanisms of self-assembly have been extensively studied. A salient feature from these examples is that hydrogen-bond-driven supramolecular polymerizations generally follow a cooperative mechanism. A closer look at these studies shows the large variation of the  $\sigma$  across different systems, although they are all driven by hydrogen-bonding. Since hydrogen-bonding is a ubiquitous interaction in both natural and synthetic molecular systems, it is paramount to understand how hydrogen-bonding relates to cooperativity in a quantitative manner. The first step in such an exercise is to determine the major contributor to the cooperativity in a system and then study the effect of monomer structure on the  $\sigma$ . Here we have initiated such a study taking the BTA family as an example to gain structural insights into the hydrogen-bonded cooperative systems. The major outcome of the present work is that the  $\sigma$  spans a continuum from isodesmic ( $\sigma = 1$ ) to highly cooperative ( $\sigma < 10^{-6}$ ) and it depends strongly on the monomer structure and correlates to hydrogen-bond strength. We anticipate that these correlations can be translated to other systems in which the self-assembly is primarily driven by intermolecular hydrogen-bond formation.<sup>9,43,44</sup> However, care should be taken in translating these correlations to systems in which other interactions influence the hydrogen-bonding. In addition, the transfer of knowledge on mechanistic aspects in organic solvents to aqueous medium is not necessarily straightforward, due to the active participation of water in the self-assembly process.



The ultimate aim of this approach would be to assign values to groups (amides, esters, alkyl chains, etc.) based on which one can predict the extent of cooperativity in a system, analogous to the classical Hammett and Taft parameters for reaction mechanisms in organic chemistry or predicting gelation behavior by solvent parameters.<sup>45</sup> To achieve this, we need a large body of data on mechanisms of different systems in which a consistent parameter such as  $\sigma$  is carefully quantified and correlated to the factor governing cooperativity (e.g., hydrogen-bonding). Thus, a leapfrog from achieving cooperativity to quantifying it and building predictive powers will positively impact the manifestations of cooperativity in synthetic systems. At present, detailed DFT calculations of the molecules designed will give a first indication of the strength of the hydrogen bonding present, and hence an indication of the level of cooperativity can be deduced.

## ■ ASSOCIATED CONTENT

### Supporting Information

The Supporting Information is available free of charge on the ACS Publications website at DOI: 10.1021/acs.accounts.7b00176.

Computation details and a list of coordinates, thermodynamic parameters of compounds 1–12, and a plot of experimentally determined  $\sigma$  values (in MCH) vs the hydrogen-bond length (PDF)

## ■ AUTHOR INFORMATION

### Corresponding Authors

\*E-mail: a.palmans@tue.nl

\*E-mail: e.w.meijer@tue.nl

### ORCID

E. W. Meijer: 0000-0003-4126-7492

Anja R. A. Palmans: 0000-0002-7201-1548

### Author Contributions

The manuscript was written through contributions of all authors. All authors have given approval to the final version of the manuscript.

### Notes

The authors declare no competing financial interest.

### Biographies

**Chidambar Kulkarni** was born in Dharwad, India. He obtained his Ph.D. degree in 2015 from JNCASR, Bangalore, on the study of mechanisms in supramolecular polymerization. Currently he is working as a Marie-Sklodowska-Curie postdoctoral fellow with Bert Meijer and Anja Palmans on supramolecular assembly of chiral semiconductors.

**Bert Meijer** was born in Groningen, the Netherlands. He studied at the University of Groningen, where he received his undergraduate degree in Chemistry in 1978 and a Ph.D. degree in 1982. During 1982–1989, he was active as a research chemist at Philips Research Laboratories in Eindhoven. From 1989 until 1992, he was head of the department “New Materials” at DSM Research in Geleen. Starting from 1991, he became full professor at the TU Eindhoven. His main research interests are the design, synthesis, characterization, and possible applications of supramolecular architectures, with special emphasis on chirality and hydrogen bonding architectures, and their use in functional materials.

**Anja Palmans** grew up in Maaseik (Belgium) and obtained a degree in chemical engineering at the TU Eindhoven (The Netherlands), followed by a Ph.D. on the topic of supramolecular chemistry (1997). After a Postdoctoral stay at the ETH Zürich (Switzerland) and working

at DSM Research (The Netherlands), she became assistant professor in at the TU Eindhoven in 2005. Since 2010, she is an associate professor focusing on the controlled folding of macromolecules and supramolecular assembly in water and organic media.

## ■ ACKNOWLEDGMENTS

The authors thank Dr. C. Schaefer for his continued support in updating the Matlab scripts to fit the temperature-dependent data. This work was financially supported by the Dutch ministry of education, culture and science (FMS Gravitation program 024.001.035). C. Kulkarni thanks Marie-Sklodowska-Curie fellowship (704830) for financial support.

## ■ REFERENCES

- (1) Brunsveld, L.; Folmer, B. J. B.; Meijer, E. W.; Sijbesma, R. P. *Supramolecular Polymers*. *Chem. Rev.* **2001**, *101*, 4071–4098.
- (2) Cordier, P.; Tournilhac, F.; Soulie-Ziakovic, C.; Leibler, L. Self-healing and thermoreversible rubber from supramolecular assembly. *Nature* **2008**, *451*, 977–980.
- (3) Aida, T.; Meijer, E. W.; Stupp, S. I. Functional Supramolecular Polymers. *Science* **2012**, *335*, 813–817.
- (4) Yang, L.; Tan, X.; Wang, Z.; Zhang, X. *Supramolecular Polymers: Historical Development, Preparation, Characterization, and Functions*. *Chem. Rev.* **2015**, *115*, 7196–7239.
- (5) De Greef, T. F. A.; Smulders, M. M. J.; Wolffs, M.; Schenning, A. P. H. J.; Sijbesma, R. P.; Meijer, E. W. *Supramolecular Polymerization*. *Chem. Rev.* **2009**, *109*, 5687–5754.
- (6) Zhao, D.; Moore, J. S. Nucleation-elongation: a mechanism for cooperative supramolecular polymerization. *Org. Biomol. Chem.* **2003**, *1*, 3471–3491.
- (7) Martin, R. B. Comparisons of Indefinite Self-Association Models. *Chem. Rev.* **1996**, *96*, 3043–3064.
- (8) Ogi, S.; Sugiyasu, K.; Manna, S.; Samitsu, S.; Takeuchi, M. Living supramolecular polymerization realized through a biomimetic approach. *Nat. Chem.* **2014**, *6*, 188–195.
- (9) Kang, J.; Miyajima, D.; Mori, T.; Inoue, Y.; Itoh, Y.; Aida, T. A rational strategy for the realization of chain-growth supramolecular polymerization. *Science* **2015**, *347*, 646–651.
- (10) Ogi, S.; Stepanenko, V.; Sugiyasu, K.; Takeuchi, M.; Würthner, F. Mechanism of Self-Assembly Process and Seeded Supramolecular Polymerization of Perylene Bisimide Organogelator. *J. Am. Chem. Soc.* **2015**, *137*, 3300–3307.
- (11) Rest, C.; Kandaneli, R.; Fernandez, G. Strategies to create hierarchical self-assembled structures via cooperative non-covalent interactions. *Chem. Soc. Rev.* **2015**, *44*, 2543–2572.
- (12) Jorgensen, W. L.; Pranata, J. Importance of secondary interactions in triply hydrogen bonded complexes: guanine-cytosine vs uracil-2,6-diaminopyridine. *J. Am. Chem. Soc.* **1990**, *112*, 2008–2010.
- (13) Hunter, C. A.; Sanders, J. K. M. The nature of  $\pi$ - $\pi$  interactions. *J. Am. Chem. Soc.* **1990**, *112*, 5525–5534.
- (14) Hunter, C. A. Quantifying Intermolecular Interactions: Guidelines for the Molecular Recognition Toolbox. *Angew. Chem. Int. Ed.* **2004**, *43*, 5310–5324.
- (15) Chen, Z.; Lohr, A.; Saha-Möller, C. R.; Würthner, F. Self-assembled  $\pi$ -stacks of functional dyes in solution: structural and thermodynamic features. *Chem. Soc. Rev.* **2009**, *38*, 564–584.
- (16) Biedermann, F.; Schneider, H.-J. Experimental Binding Energies in Supramolecular Complexes. *Chem. Rev.* **2016**, *116*, 5216–5300.
- (17) Kulkarni, C.; Balasubramanian, S.; George, S. J. What Molecular Features Govern the Mechanism of Supramolecular Polymerization? *ChemPhysChem* **2013**, *14*, 661–673.
- (18) Hunter, C. A.; Anderson, H. L. What is Cooperativity? *Angew. Chem. Int. Ed.* **2009**, *48*, 7488–7499.
- (19) Cantekin, S.; de Greef, T. F. A.; Palmans, A. R. A. Benzene-1,3,5-tricarboxamide: a versatile ordering moiety for supramolecular chemistry. *Chem. Soc. Rev.* **2012**, *41*, 6125–6137.

(20) Smulders, M. M. J.; Nieuwenhuizen, M. M. L.; de Greef, T. F. A.; van der Schoot, P.; Schenning, A. P. H. J.; Meijer, E. W. How to Distinguish Isodesmic from Cooperative Supramolecular Polymerisation. *Chem. - Eur. J.* **2010**, *16*, 362–367.

(21) Jonkheijm, P.; van der Schoot, P.; Schenning, A. P. H. J.; Meijer, E. W. Probing the Solvent-Assisted Nucleation Pathway in Chemical Self-Assembly. *Science* **2006**, *313*, 80–83.

(22) Markvoort, A. J.; ten Eikelder, H. M. M.; Hilbers, P. A. J.; de Greef, T. F. A.; Meijer, E. W. Theoretical models of nonlinear effects in two-component cooperative supramolecular copolymerizations. *Nat. Commun.* **2011**, *2*, 509.

(23) ten Eikelder, H. M. M.; Markvoort, A. J.; de Greef, T. F. A.; Hilbers, P. A. J. An Equilibrium Model for Chiral Amplification in Supramolecular Polymers. *J. Phys. Chem. B* **2012**, *116*, 5291–5301.

(24) Lightfoot, M. P.; Mair, F. S.; Pritchard, R. G.; Warren, J. E. New supramolecular packing motifs:  $\pi$ -stacked rods encased in triply-helical hydrogen bonded amide strands. *Chem. Commun.* **1999**, 1945–1946.

(25) Smulders, M. M. J.; Schenning, A. P. H. J.; Meijer, E. W. Insight into the Mechanisms of Cooperative Self-Assembly: The “Sergeants-and-Soldiers” Principle of Chiral and Achiral  $C_3$ -Symmetrical Discotic Triamides. *J. Am. Chem. Soc.* **2008**, *130*, 606–611.

(26) Pilot, I. A. W.; Palmans, A. R. A.; Hilbers, P. A. J.; van Santen, R. A.; Pidko, E. A.; de Greef, T. F. A. Understanding Cooperativity in Hydrogen-Bond-Induced Supramolecular Polymerization: A Density Functional Theory Study. *J. Phys. Chem. B* **2010**, *114*, 13667–13674.

(27) Bejagam, K. K.; Balasubramanian, S. Supramolecular Polymerization: A Coarse Grained Molecular Dynamics Study. *J. Phys. Chem. B* **2015**, *119*, 5738–5746.

(28) Stals, P. J. M.; Smulders, M. M. J.; Martín-Rapún, R.; Palmans, A. R. A.; Meijer, E. W. Asymmetrically Substituted Benzene-1,3,5-tricarboxamides: Self-Assembly and Odd–Even Effects in the Solid State and in Dilute Solution. *Chem. - Eur. J.* **2009**, *15*, 2071–2080.

(29) Nakano, Y.; Hirose, T.; Stals, P. J. M.; Meijer, E. W.; Palmans, A. R. A. Conformational analysis of supramolecular polymerization processes of disc-like molecules. *Chem. Sci.* **2012**, *3*, 148–155.

(30) Cantekin, S.; Nakano, Y.; Everts, J. C.; van der Schoot, P.; Meijer, E. W.; Palmans, A. R. A. A stereoselectively deuterated supramolecular motif to probe the role of solvent during self-assembly processes. *Chem. Commun.* **2012**, *48*, 3803–3805.

(31) Cook, J. L.; Hunter, C. A.; Low, C. M. R.; Perez-Velasco, A.; Vinter, J. G. Solvent Effects on Hydrogen Bonding. *Angew. Chem., Int. Ed.* **2007**, *46*, 3706–3709.

(32) Nakano, Y.; Markvoort, A. J.; Cantekin, S.; Pilot, I. A. W.; ten Eikelder, H. M. M.; Meijer, E. W.; Palmans, A. R. A. Conformational Analysis of Chiral Supramolecular Aggregates: Modeling the Subtle Difference between Hydrogen and Deuterium. *J. Am. Chem. Soc.* **2013**, *135*, 16497–16506.

(33) Palmans, A. R. A.; Vekemans, J. A. J. M.; Havinga, E. E.; Meijer, E. W. Sergeants-and-Soldiers Principle in Chiral Columnar Stacks of Disc-Shaped Molecules with  $C_3$  Symmetry. *Angew. Chem., Int. Ed. Engl.* **1997**, *36*, 2648–2651.

(34) Metzroth, T.; Hoffmann, A.; Martin-Rapun, R.; Smulders, M. M. J.; Pieterse, K.; Palmans, A. R. A.; Vekemans, J. A. J. M.; Meijer, E. W.; Spiess, H. W.; Gauss, J. Unravelling the fine structure of stacked bipyridine diamine-derived  $C_3$ -discotics as determined by X-ray diffraction, quantum-chemical calculations, Fast-MAS NMR and CD spectroscopy. *Chem. Sci.* **2011**, *2*, 69–76.

(35) Palmans, A. R. A.; Vekemans, J. A. J. M.; Fischer, H.; Hikmet, R. A.; Meijer, E. W. Extended-Core Discotic Liquid Crystals Based on the Intramolecular H-Bonding in N-Acylated 2,2'-Bipyridine-3,3'-diamine Moieties. *Chem. - Eur. J.* **1997**, *3*, 300–307.

(36) Cantekin, S.; ten Eikelder, H. M. M.; Markvoort, A. J.; Veld, M. A. J.; Korevaar, P. A.; Green, M. M.; Palmans, A. R. A.; Meijer, E. W. Consequences of Cooperativity in Racemizing Supramolecular Systems. *Angew. Chem., Int. Ed.* **2012**, *51*, 6426–6431.

(37) Veld, M. A. J.; Haveman, D.; Palmans, A. R. A.; Meijer, E. W. Sterically demanding benzene-1,3,5-tricarboxamides: tuning the mechanisms of supramolecular polymerization and chiral amplification. *Soft Matter* **2011**, *7*, 524–531.

(38) Desmarchelier, A.; Alvarenga, B. G.; Caumes, X.; Dubreucq, L.; Troufflard, C.; Tessier, M.; Vanthuyne, N.; Ide, J.; Maistriau, T.; Beljonne, D.; Brocorens, P.; Lazzaroni, R.; Raynal, M.; Bouteiller, L. Tuning the nature and stability of self-assemblies formed by ester benzene 1,3,5-tricarboxamides: the crucial role played by the substituents. *Soft Matter* **2016**, *12*, 7824–7838.

(39) Stals, P. J. M.; Everts, J. C.; de Bruijn, R.; Pilot, I. A. W.; Smulders, M. M. J.; Martín-Rapún, R.; Pidko, E. A.; de Greef, T. F. A.; Palmans, A. R. A.; Meijer, E. W. Dynamic Supramolecular Polymers Based on Benzene-1,3,5-tricarboxamides: The Influence of Amide Connectivity on Aggregate Stability and Amplification of Chirality. *Chem. - Eur. J.* **2010**, *16*, 810–821.

(40) van Herrikhuyzen, J.; Jonkheijm, P.; Schenning, A. P. H. J.; Meijer, E. W. The influence of hydrogen bonding and  $\pi$ - $\pi$  stacking interactions on the self-assembly properties of  $C_3$ -symmetrical oligo(p-phenylenevinylene) discs. *Org. Biomol. Chem.* **2006**, *4*, 1539–1545.

(41) Reiner, A.; Wildemann, D.; Fischer, G.; Kiefhaber, T. Effect of Thiopeptide Bonds on  $\alpha$ -Helix Structure and Stability. *J. Am. Chem. Soc.* **2008**, *130*, 8079–8084.

(42) Mes, T.; Cantekin, S.; Balkenende, D. W. R.; Frissen, M. M. M.; Gillissen, M. A. J.; De Waal, B. F. M.; Voets, I. K.; Meijer, E. W.; Palmans, A. R. A. Thioamides: Versatile Bonds To Induce Directional and Cooperative Hydrogen Bonding in Supramolecular Polymers. *Chem. - Eur. J.* **2013**, *19*, 8642–8649.

(43) García, F.; Viruela, P. M.; Matesanz, E.; Ortí, E.; Sánchez, L. Cooperative Supramolecular Polymerization and Amplification of Chirality in  $C_3$ -Symmetrical OPE-Based Trisamides. *Chem. - Eur. J.* **2011**, *17*, 7755–7759.

(44) Helmich, F.; Lee, C. C.; Nieuwenhuizen, M. M. L.; Gielen, J. C.; Christianen, P. C. M.; Larsen, A.; Fytas, G.; Leclère, P. E. L. G.; Schenning, A. P. H. J.; Meijer, E. W. Dilution-Induced Self-Assembly of Porphyrin Aggregates: A Consequence of Coupled Equilibria. *Angew. Chem., Int. Ed.* **2010**, *49*, 3939–3942.

(45) Lan, Y.; Corradini, M. G.; Weiss, R. G.; Raghavan, S. R.; Rogers, M. A. To gel or not to gel: correlating molecular gelation with solvent parameters. *Chem. Soc. Rev.* **2015**, *44*, 6035–6058.